Atomic layer deposition of aluminum fluoride using $Al(CH_3)_3$ and SF_6 plasma

Atomic layer deposition of aluminum fluoride using $Al(CH_3)_3$ and SF_6 plasma

M. F. J. Vos, H. C. M. Knoops, R. A. Synowicki, W. M. M. Kessels, and A. J. M. Mackus

Citation: Appl. Phys. Lett. **111**, 113105 (2017); doi: 10.1063/1.4998577
View online: http://dx.doi.org/10.1063/1.4998577
View Table of Contents: http://aip.scitation.org/toc/apl/111/11
Published by the American Institute of Physics

Atomic layer deposition of aluminum fluoride using $Al(CH_3)_3$ and SF_6 plasma

M. F. J. Vos,[1,a)] H. C. M. Knoops,[1,2] R. A. Synowicki,[3] W. M. M. Kessels,[1] and A. J. M. Mackus[1,a)]
[1]*Department of Applied Physics, Eindhoven University of Technology, P.O. Box 513, 5600 MB Eindhoven, The Netherlands*
[2]*Oxford Instruments Plasma Technology, North End, Bristol BS49 4AP, United Kingdom*
[3]*J.A. Woollam Co., Inc., 645 M Street, Suite 102, Lincoln, Nebraska 68508, USA*

(Received 1 August 2017; accepted 1 September 2017; published online 15 September 2017)

Metal fluorides typically have a low refractive index and a very high transparency and find many applications in optical and optoelectronic devices. Nearly stoichiometric, high-purity AlF_3 films were deposited by atomic layer deposition (ALD) using trimethylaluminum [$Al(CH_3)_3$] and SF_6 plasma. Self-limiting growth was confirmed and the growth per cycle was determined to range from 1.50 Å to 0.55 Å for deposition temperatures between 50 °C and 300 °C. In addition, the film density of $\sim 2.8\ g\,cm^{-3}$ was found to be relatively close to the bulk value of $3.1\ g\,cm^{-3}$. Vacuum ultraviolet spectroscopic ellipsometry measurements over the wavelength range of 140–2275 nm showed a refractive index n of 1.35 at 633 nm, and an extinction coefficient k of $<10^{-4}$ above 300 nm, for all deposition temperatures. Optical emission spectroscopy during the SF_6 plasma exposure step of the ALD cycle revealed the formation of C_2H_2 and CF_2 species, resulting from the interaction of the plasma with the surface after $Al(CH_3)_3$ exposure. On the basis of these results, a reaction mechanism is proposed in which F radicals from the SF_6 plasma participate in the surface reactions. Overall, this work demonstrates that SF_6 plasma is a promising co-reactant for ALD of metal fluorides, providing an alternative to co-reactants such as metal fluorides, HF, or HF-pyridine. *Published by AIP Publishing*. [http://dx.doi.org/10.1063/1.4998577]

Metal fluorides such as AlF_3, MgF_2, and CaF_2 generally have a wide bandgap (>10 eV) and low refractive index (1.3–1.6).[1–4] Due to these properties, they find use in many optical devices, including waveguides, Bragg reflectors, optical filters, and mirrors.[5–9] Moreover, metal fluorides have been used as electron-selective contacts in photovoltaics and protective layers in Li-ion batteries.[10–12] Thin metal fluoride films have been deposited using a variety of techniques such as sputtering, evaporation, and more recently atomic layer deposition (ALD).

ALD is a chemical vapor deposition technique that is based on alternating precursor and co-reactant exposures. Compared to other deposition techniques, ALD offers the benefits of precise thickness control and the ability to deposit uniform and conformal films on large-area substrates.[13] These merits can facilitate applications of metal fluorides such as 3D-nanostructured optical devices and batteries. Mostly, metal oxides have been explored by ALD, often using H_2O, O_3, or O_2 plasma as the co-reactant.[14] Metal nitrides have also been studied extensively, in this case mainly with NH_3 gas or H_2, N_2, and NH_3-based plasmas. The choice of co-reactant is not only important for determining the type of material that is deposited (oxide, nitride, etc.) but also since it often affects the deposition conditions (such as deposition temperature) and the threshold for industrial implementation. In this respect, ALD of metal fluorides is more challenging, due to limited choice of suitable co-reactants. Previously, ALD of fluorides has been demonstrated using TiF_4 and TaF_5 as the F-source for the deposition of AlF_3, MgF_2, CaF_2, LiF, and LaF_3, which can be accompanied by Ti or Ta incorporation.[15–19] More recently, AlF_3, ZrF_4, MnF_2, HfF_2, MgF_2, and ZnF_2 have been deposited by HF either using pure HF or a HF-pyridine solution.[8,9,20,21] Lee *et al.* gave insight into the reaction mechanisms during ALD using HF as the co-reactant and postulated that HF adsorbed on the surface serves as the reactive sites for the precursor molecules to bind.[20,21] Moreover, Dumont and George found that the temperature dependence of the growth per cycle (GPC) can be explained by the amount of HF adsorbed on AlF_3, which decreases with temperature.[22]

In this work, SF_6 plasma was explored as the co-reactant for ALD of metal fluorides. Using trimethylaluminum [TMA, $Al(CH_3)_3$] as precursor and SF_6 plasma as F-source, high-purity AlF_3 films were deposited in an Oxford Instruments FlexAL™ ALD reactor. It is demonstrated that this approach is a promising alternative to HF or HF-pyridine as co-reactant. As compared to thermal ALD, the use of a plasma as co-reactant generally allows for an increased GPC at lower temperatures, reduction of the purge times, and additional control over the material properties.[23] SF_6 is a stable, non-toxic gas that is relatively easy to handle and therefore commonly applied. The dominant neutral species in an inductively coupled SF_6 plasma are known to be SF_6, F, F_2, and SF_4, while the dominant ions are SF_5^+ and F^-.[24–26] The concentration of S and S^+ is typically a factor $\sim 10^3$ lower than the concentration of F and F^-.[25] SF_6 plasmas, as well as other F-containing plasmas such as CF_4 and NF_3, are extensively used for etching (Si, SiO_2, Si_3N_4, …) and chamber cleaning, meaning that the existing knowledge can be utilized for ALD process development. Moreover,

a)Authors to whom correspondence should be addressed: m.f.j.vos@tue.nl and a.j.m.mackus@tue.nl.

F-based plasmas are widely available both in research and manufacturing, which can facilitate the implementation and scale-up of plasma ALD of metal fluorides.[27]

To confirm ALD behavior, the GPC was determined using *in situ* spectroscopic ellipsometry (SE) as a function of TMA dosing time, plasma exposure time, and purge times at a deposition temperature of 200 °C.[28] The saturation curve for the plasma exposure time in Fig. 1 clearly indicates saturation around 5–10 s. 20 cycles of Al_2O_3 ALD were performed prior to AlF_3 deposition to prevent etching of the Si (100) substrate (see supplementary material). The GPC as a function of precursor dosing time was found to saturate after 40 ms, and self-limiting behavior was also confirmed as a function of both purge times and for a deposition temperature of 50 °C (supplementary material, Fig. S1). Based on the saturation curves, a TMA dose of 80 ms, followed by a purge step of 6 s, a plasma exposure of 10 s, and a final purge step of 4 s were used for the remainder of the experiments.

The uniformity and conformality were investigated (without additional optimization) to further demonstrate the ALD behavior of the process. Using SE-mapping of a film deposited on a 200 mm wafer, the thickness and refractive index non-uniformity (standard deviation, 1 sigma) were determined to be 3.9% and 0.3%, respectively, which indicates good uniformity (see supplementary material, Fig. S2). The conformality was studied by depositing AlF_3 on a GaP nanowire array and analyzing separated nanowires using transmission electron microscopy (TEM). The ~7 μm long nanowires were randomly located on the substrate, spaced at 0 nm–500 nm (meaning that the ratio between the length and spacing is 14 or higher). The TEM pictures in the inset of Fig. 1 clearly show a conformal, ~20 nm thick film along the full length of a nanowire (see also Fig. S3, supplementary material). The ratio between the thickness at the bottom and the top of the nanowire was determined to be >0.9, indicating a SF_6 plasma can enable conformal deposition on 3D structures.

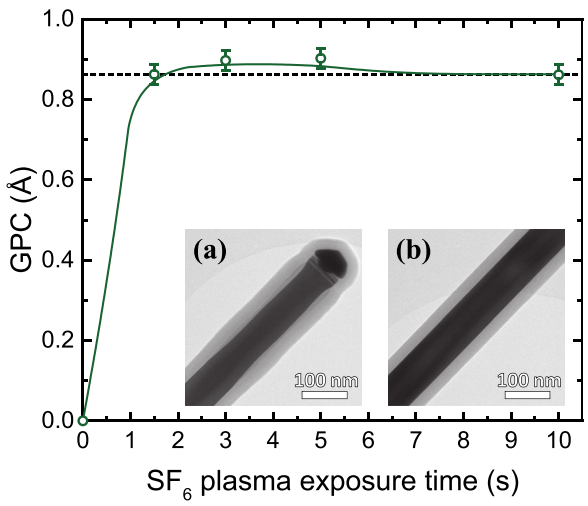

FIG. 1. Growth per cycle (GPC) as a function of plasma exposure time for a precursor dosing time of 40 ms and a deposition temperature of 200 °C. The line serves as a guide to the eye. Inset: TEM images of (a) the top and (b) the middle of a GaP nanowire (~7 μm in length) after deposition of a ~20 nm AlF_3 film at 200 °C, illustrating the conformality of the ALD process.

The effect of the table temperature on the growth of the AlF_3 films was investigated by depositing films at temperatures of 50 °C, 100 °C, 200 °C, and 300 °C. The thickness as a function of ALD cycles in the inset of Fig. 2 shows a linear behavior for all temperatures as is expected for ALD. The GPC in terms of thickness as determined from SE in Fig. 2 is strongly dependent on the table temperature and decreases from 1.50 Å for a temperature of 50 °C to 0.55 Å for 300 °C. The GPC in terms of Al atoms deposited per nm^{-2} as determined from Rutherford backscattering spectroscopy (RBS) follows a similar trend. This indicates that the decrease in GPC is not caused by an increased atomic density at higher temperatures, but rather by reduced precursor adsorption. The decrease in GPC with temperature is similar to the observations by Lee *et al.* and Hennessy *et al.* for thermal ALD of AlF_3 using HF as co-reactant.[9,20] This trend is likely related to a reduced amount of HF adsorbed on the surface at higher temperatures, leading to decreased TMA adsorption in the precursor half-cycle, which is analogous to dehydroxylation for metal oxide ALD.[22] A transition from AlF_3 ALD to Al_2O_3 atomic layer etching (ALE) at temperatures above 250 °C, as found by Lee *et al.*, was however not observed. This difference can be explained by the fact that our actual sample temperature is lower than the set table temperature due to reduced thermal contact in vacuum (see also the supplementary material).

Table I summarizes the properties of the AlF_3 films as determined by a combination of SE, RBS, and elastic recoil detection (ERD) measurements. No significant impurity levels of S, O, and C were detected in the AlF_3 films using RBS, even for low deposition temperatures. The S-content was found to be 0.5 at. % for a deposition temperature of 50 °C and decreased to below the detection limit for 300 °C. The minimal amount of S incorporation can be explained by the difference in reactivity of F and S. From a comparison of the electronegativity and electron affinity of F and S it becomes evident that it is much more likely to incorporate F.[29,30] Furthermore, RBS measurements showed a F/Al ratio of 2.9–3.1 and an O content of around 0.5–1 at. %. From ERD, the H content of the AlF_3 films was determined to be between 3.2 at. % and 1.3 at. %. These results are in

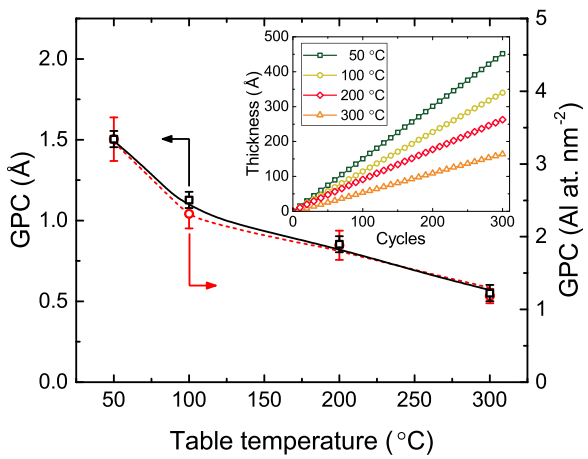

FIG. 2. Growth per cycle (GPC) as a function of substrate table temperature in terms of thickness as determined from SE (left axis) and deposited Al atoms per nm^2 as measured by RBS (right axis). The lines serve as guides to the eye. Inset: Thickness as a function of ALD cycles for deposition temperatures between 50 °C and 300 °C.

TABLE I. Properties of AlF_3 films for deposition temperatures between 50 °C and 300 °C. The growth per cycle (GPC) in terms of Al atoms $nm^{-2}cycle^{-1}$ and the chemical composition were determined from RBS and ERD, the refractive index from VUV-SE, and the mass density by combining the RBS and SE results. Typical errors are indicated in the top row, unless the error varies with temperature.

Deposition temperature (°C)	GPC (Å)	GPC (Al at. nm^{-2})	F/Al	[S] (at. %)	[H] (at. %)	Mass density ($g{\cdot}cm^{-3}$)	Refractive index
50	1.50 ± 0.05	3.3 ± 0.3	3.1 ± 0.5	0.5 ± 0.1	3.2 ± 0.8	2.8 ± 0.3	1.35 ± 0.01
100	1.13	2.3 ± 0.2	3.1	0.3	2.3 ± 0.5	2.7	1.34
200	0.85	1.9 ± 0.2	2.9	0.2	1.7 ± 0.3	2.9	1.35
300	0.55	1.2 ± 0.1	2.9	0.0	1.3 ± 0.2	2.7	1.35

agreement with XPS measurements (see supplementary material, Fig. S4). Using the RBS, ERD, and SE data, the density of the films was calculated to be between 2.7 g cm^{-3} and 2.9 g cm^{-3}, which is relatively close to the AlF_3 bulk value of 3.1 g cm^{-3}. Moreover, atomic force microscopy (AFM) measurements indicated very smooth films with root mean square (RMS) roughness values ≤0.2 nm (see supplementary material, Fig. S5). Grazing-incidence X-ray diffraction (XRD) measurements revealed that the films were amorphous for all deposition temperatures (see supplementary material, Fig. S6). Note that the obtained properties are very similar to the results reported for AlF_3 ALD using HF as co-reactant.[20]

Figure 3 shows the optical properties as obtained from vacuum ultraviolet (VUV)-SE measurements for an AlF_3 film deposited at 200 °C.[31] The refractive index n is ∼1.35 at 633 nm (1.96 eV), and the film shows a relatively low dispersion (i.e., a weak dependence of n on wavelength). The refractive index values for the other deposition temperatures are similar with values between 1.34 and 1.36 at 633 nm [see supplementary material, Fig. S7(a)]. The extinction coefficient k is $<10^{-6}$ over the wavelength range of 300–2275 nm for a deposition temperature of 200 °C (Fig. 3). Moreover, the inset of Fig. 3 shows low absorption for all other deposition temperatures, i.e., $<10^{-4}$ below photon energies of 4.1 eV (wavelengths >300 nm). The extinction coefficient for 50 °C is higher than for 100 °C and 200 °C, which might be related to a higher S content at 50 °C. The reason for the increased absorption for 300 °C is currently not understood and requires additional investigation. To obtain a good fit to the data, a Tauc-Lorentz and two Gaussian oscillators were needed to describe the dielectric function. The two Gaussian oscillators used to fit the absorption below the band gap are visible at photon energies around 6.4 eV and 7.8 eV (inset Fig. 3). The presence of an absorption band around 6.4 eV was previously observed by Barrière and Lachter.[1] Note that the band gap (>10 eV) cannot be determined from the VUV-SE data since it lies above the maximum photon energy of 8.8 eV. The refractive index values of ∼1.35 are in agreement with AlF_3 films prepared by ALD using HF and TiF_4 as the co-reactants.[16,20] Moreover, the obtained n and k values are close to what can be expected for AlF_3 and indicate that SF_6 plasma enables ALD of high-quality metal fluoride films.[1–3]

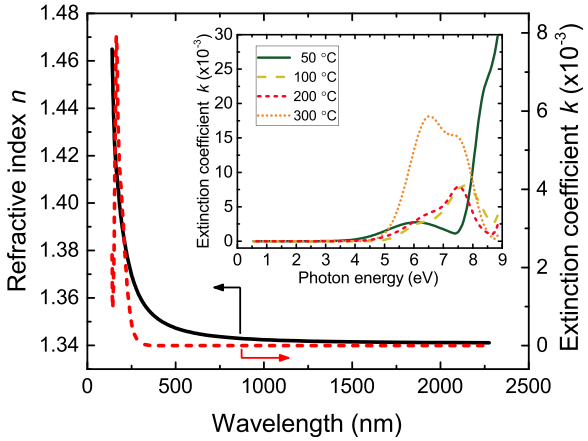

FIG. 3. Refractive index n and extinction coefficient k as a function of wavelength as determined from VUV-SE for a ∼35 nm thick film deposited at a temperature of 200 °C. Inset: Extinction coefficient k as a function of photon energy for deposition temperatures between 50 °C and 300 °C.

To get more insight into the SF_6 plasma as co-reactant for ALD, Fig. 4 shows optical emission spectrometry (OES) data collected during a steady-state SF_6 plasma (no ALD, i.e., without preceding TMA dosing) and during the plasma exposure step of an AlF_3 ALD cycle (i.e., after TMA dosing).[32] Comparison of the two spectra gives insight in the consumption and formation of species during the plasma exposure step of the ALD cycle. The spectrum for the normal SF_6 plasma is dominated by characteristic lines for F at 685.6 nm, 703.7 nm, and 739.9 nm.[33] In addition, the SF_x band starting at 289.3 nm and the S-lines at 469.4 nm, 545.4 nm, and 564.0 nm can be identified.[33,34] Furthermore, H-lines at 486.1 nm and 656.3 nm are present, which can be attributed to residual background species (e.g., H_2O) in the plasma.[33] In the OES spectrum collected during an ALD cycle (after TMA dosing), additional lines are visible around 250 nm–300 nm, indicating the formation of C_2H_2 and CF_2 as reaction products.[35–38] Moreover, this spectrum shows a decreased intensity for the F-lines, implying consumption of F, and an increased intensity for the H-lines, related to excitation of hydrogen from the methyl groups (see supplementary material, Fig. S8 for a zoomed view of the region between 650 nm and 800 nm). These observations indicate that F radicals react with methyl surface groups during the SF_6 plasma exposure step, which leads to the formation of hydrofluorocarbons (CH_yF_{4-y}), both in surface and plasma reactions. The presence of C_2H_2 can be explained by the reaction of hydrofluorocarbons in the plasma (see below).[39] Based on these findings, and on the work of Lee *et al.*,[20] the following reactions can be proposed for the two half-cycles:

$$HF_{(ads)} + Al(CH_3)_{3\,(g)} \rightarrow AlF(CH_3)_{2\,(ads)} + CH_{4\,(g)}, \quad (1a)$$

$$AlF(CH_3)_{2\,(ads)} + F_{(g)} \rightarrow AlF_{3\,(s)} + HF_{(ads,g)} + CH_yF_{4-y\,(g)}. \quad (1b)$$

For simplicity, these equations are written unbalanced, and it is assumed that the hydrofluorocarbon species (CH_yF_{4-y})

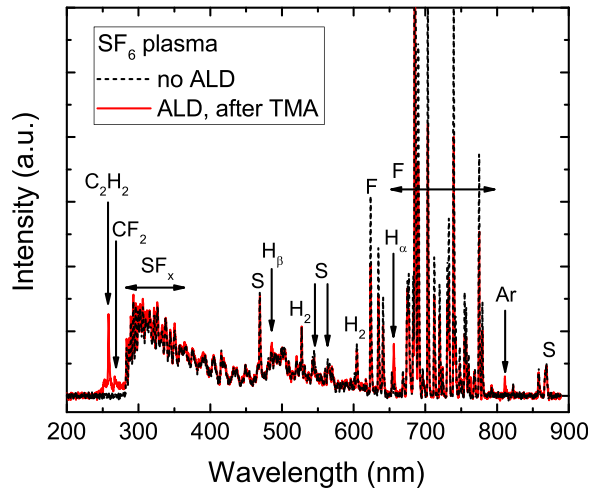

FIG. 4. Optical emission spectra of a SF_6 plasma ("no ALD") and a SF_6 plasma during an AlF_3 ALD cycle ("ALD, after TMA"). In the latter case, in addition to lines related to the SF_6 plasma and reaction products, an Ar line is visible at 811.5 nm, which is due to Ar residing in the chamber after the preceding purge step. The SF_6 gas flow was set to 50 sccm (instead of 100 sccm) to increase the residence time of the species in the plasma.

contain only one C atom with $0 \leq y \leq 3$. In the first half-cycle [Eq. (1a)], the TMA molecule reacts with HF adsorbed on the surface, releasing CH_4 as product.[20] In this way, the density of HF on the surface determines the amount of TMA precursor adsorption. The temperature dependence of the HF surface density can thus explain the decrease of GPC with temperature.[22] Note that Eq. (1a) states that one methyl group is eliminated upon precursor adsorption, although removal of two or three methyl groups may also be possible. In the plasma half-cycle [Eq. (1b)], the adsorbed $AlF(CH_3)_2$ reacts with F radicals from the plasma, forming HF, which partly remains on the surface, and CH_yF_{4-y} species, which are released from the surface and end up in the plasma where they can be dissociated and form other species. The reaction mechanism for thermal ALD with HF is different, as only CH_4 is produced in both half-cycles.[20] Note that the release of CH_4 ($y = 4$) as a reaction product in the SF_6 plasma half-cycle requires a source of H, such as HF. However, HF is formed according to reaction (1b) and can enable a secondary, thermal reaction pathway, resulting in the release of CH_4. This CH_4 can subsequently react in the plasma to form C_2H_2.[39] It is noted that the presence of HF, CH_4, C_2H_2, and CH_yF_{4-y} species was corroborated using quadrupole mass spectrometry (see supplementary material Fig. S9), as will be discussed in more detail in a follow-up publication.

In conclusion, it was demonstrated that the ALD process using TMA and SF_6 plasma yields high-purity, nearly stoichiometric AlF_3 films. Self-limiting behavior was confirmed for all process steps, and the GPC was found to decrease with temperature. In addition, material properties such as density and refractive index were found to be in line with literature reports on AlF_3. A reaction mechanism was proposed where F radicals remove the CH_3-ligands and bind to Al to form AlF_3. CH_4 is released as a reaction product in the precursor half-cycle, whereas HF and hydrofluorocarbons are released during the plasma exposure. Considering the high reactivity of SF_6 plasma and the low amount of S incorporation in the films, SF_6 plasma can likely be used as the co-reactant for ALD of other metal fluorides such as MgF_2, LiF, and CaF_2. Moreover, it can be expected that NF_3 can be used similarly. The wide availability and the ease of handling of these gases make plasma ALD of metal fluorides feasible on a wide scale.

See supplementary material for the detailed description of the experimental conditions and additional data on the ALD behavior and the material properties.

This work was financially supported by the *Zwaartekracht* program of the Netherlands Organisation for Scientific Research (NWO). The authors gratefully acknowledge C. A. A. van Helvoirt and J. van Gerwen for technical assistance and A. Kurek from Oxford Instruments Plasma Technology for performing the SE-mapping measurements. The authors would also like to thank Dr. S. Assali and L. Gagliano for providing the GaP nanowires and Dr. M. A. Verheijen for the TEM analysis. Solliance and the Dutch province of Noord-Brabant are acknowledged for funding the TEM facility.

[1]A. S. Barrière and A. Lachter, Appl. Opt. **16**, 2865 (1977).
[2]J. Sun, X. Li, W. Zhang, K. Yi, and J. Shao, Appl. Opt. **51**, 8481 (2012).
[3]B.-H. Liao, M.-C. Liu, and C.-C. Lee, Appl. Opt. **47**, C41 (2008).
[4]J. D. Traylor Kruschwitz and W. T. Pawlewicz, Appl. Opt. **36**, 2157 (1997).
[5]L. Zhang, J. Zhao, P. Liu, T. Liu, Y. Zhou, X. Yu, and X. Wang, J. Lightwave Technol. **33**, 2228 (2015).
[6]M. Muallem, A. Palatnik, G. D. Nessim, and Y. R. Tischler, ACS Appl. Mater. Interfaces **7**, 474 (2015).
[7]G. Kedawat, S. Srivastava, V. K. Jain, P. Kumar, V. Kataria, Y. Agrawal, B. K. Gupta, and Y. K. Vijay, ACS Appl. Mater. Interfaces **5**, 4872 (2013).
[8]J. Hennessy, A. D. Jewell, F. Greer, M. C. Lee, and S. Nikzad, J. Vac. Sci. Technol., A **33**, 01A125 (2015).
[9]J. Hennessy, A. D. Jewell, K. Balasubramanian, and S. Nikzad, J. Vac. Sci. Technol., A **34**, 01A120 (2016).
[10]Y. Wan, C. Samundsett, J. Bullock, T. Allen, M. Hettick, D. Yan, P. Zheng, X. Zhang, J. Cui, J. McKeon, A. Javey, and A. Cuevas, ACS Appl. Mater. Interfaces **8**, 14671 (2016).
[11]S. M. Sultan, K. Sun, O. D. Clark, T. B. Masaud, Q. Fang, R. Gunn, J. Partridge, M. W. Allen, P. Ashburn, and H. M. H. Chong, IEEE Electron Device Lett. **33**, 203 (2012).
[12]F. Ding, W. Xu, D. Choi, W. Wang, X. Li, M. H. Engelhard, X. Chen, Z. Yang, and J.-G. Zhang, J. Mater. Chem. **22**, 12745 (2012).
[13]S. M. George, Chem. Rev. **110**, 111 (2010).
[14]R. W. Johnson, A. Hultqvist, and S. F. Bent, Mater. Today **17**, 236 (2014).
[15]M. Mäntymäki, J. Hämäläinen, E. Puukilainen, F. Munnik, M. Ritala, and M. Leskelä, Chem. Vap. Deposition **19**, 111 (2013).
[16]M. Mäntymäki, M. J. Heikkilä, E. Puukilainen, K. Mizohata, B. Marchand, J. Räisänen, M. Ritala, and M. Leskelä, Chem. Mater. **27**, 604 (2015).
[17]T. Pilvi, T. Hatanpää, E. Puukilainen, K. Arstila, M. Bischoff, U. Kaiser, N. Kaiser, M. Leskelä, and M. Ritala, J. Mater. Chem. **17**, 5077 (2007).
[18]T. Pilvi, E. Puukilainen, U. Kreissig, M. Leskelä, and M. Ritala, Chem. Mater. **20**, 5023 (2008).
[19]T. Pilvi, M. Ritala, M. Leskelä, M. Bischoff, U. Kaiser, and N. Kaiser, Appl. Opt. **47**, C271 (2008).
[20]Y. Lee, J. W. DuMont, A. S. Cavanagh, and S. M. George, J. Phys. Chem. C **119**, 14185 (2015).
[21]Y. Lee, H. Sun, M. J. Young, and S. M. George, Chem. Mater. **28**, 2022 (2016).
[22]J. W. DuMont and S. M. George, J. Chem. Phys. **146**, 052819 (2017).
[23]H. B. Profijt, S. E. Potts, M. C. M. van de Sanden, and W. M. M. Kessels, J. Vac. Sci. Technol., A **29**, 50801 (2011).
[24]G. Kokkoris, A. Panagiotopoulos, A. Goodyear, M. Cooke, and E. Gogolides, J. Phys. D: Appl. Phys. **42**, 55209 (2009).
[25]M. Mao, Y. Wang, and A. Bogaerts, J. Phys. D: Appl. Phys. **44**, 435202 (2011).

[26]S. Oh, H. Lee, C. Chung, S. Oh, H. Lee, and C. Chung, Phys. Plasmas **24**, 13512 (2017).
[27]R. D'Agostino and D. L. Flamm, J. Appl. Phys. **52**, 162 (1981).
[28]E. Langereis, S. B. S. Heil, H. C. M. Knoops, W. Keuning, M. C. M. van de Sanden, and W. M. M. Kessels, J. Phys. D: Appl. Phys. **42**, 73001 (2009).
[29]Y.-R. Luo, *Comprehensive Handbook of Chemical Bond Energies* (CRC-Press, Boca Raton, FL, 2007).
[30]F has an electronegativity and electron affinity of 3.98 and 328 kJ/mol respectively, as compared to 2.58 and 200 kJ/mol for S.
[31]J. N. Hilfiker, C. L. Bungay, R. A. Synowicki, T. E. Tiwald, C. M. Herzinger, B. Johs, G. K. Pribil, and J. A. Woollam, J. Vac. Sci. Technol., A **21**, 1103 (2003).
[32]A. J. M. Mackus, S. B. S. Heil, E. Langereis, H. C. M. Knoops, M. C. M. van de Sanden, and W. M. M. Kessels, J. Vac. Sci. Technol., A **28**, 77 (2010).
[33]J. E. Sansonetti and W. C. Martin, J. Phys. Chem. Ref. Data **34**, 1559 (2005).
[34]Z. L. Petrović, F. Tochikubo, S. Kakuta, and T. Makabe, J. Appl. Phys. **73**, 2163 (1993).
[35]R. W. B. Gaydon and A. G. Pearse, *The Identification of Molecular Spectra* (Chapman & Hall, London, 1950).
[36]C. B. Labelle and K. K. Gleason, J. Appl. Polym. Sci. **80**, 2084 (2001).
[37]S. F. Durrant, R. P. Mota, and M. A. Bica De Moraes, J. Appl. Phys. **71**, 448 (1992).
[38]O. V. Proshina, T. V. Rakhimova, D. V. Lopaev, V. Šamara, M. R. Baklanov, and J.-F. de Marneffe, Plasma Sources Sci. Technol. **24**, 55006 (2015).
[39]A. Majumdar, F. Behnke, R. Hippler, K. Matyash, and R. Schneider, J. Phys. Chem. A **109**, 9371 (2005).